Performance Analysis of 12Slot-14Pole for HEFSM and FEFSM with Outer-Rotor Configuration

[1]M. Z. Ahmad, [2]S. M. N. S. Othman, [3]M. M. A. Mazlan, [4]E. Sulaiman

Dept. of Electrical Power Engineering
UniversitiTun Hussein Onn Malaysia
86400 Parit Raja, Johor, MALAYSIA

[1]zarafi@uthm.edu.my, [2]ge130092@siswa.uthm.edu.my, [3]mubinaizat@gmail.com, [4]erwan@uthm.edu.my,

***Abstract*- This paper presents the performance analysis of 12Slot-14Pole for hybrid excitation flux switching machine (HEFSM) and field excitation flux switching machine(FEFSM) with outer-rotor configuration. Nowadays, research on flux switching machines (FSMs) become an attractive research topic due to several excessive advantages of robust rotor structure, high torque and power capability, and low manufacturing cost that suitable for heavy applications. The FSMs that constructed with two flux sources namely permanent magnet (PM) and flux excitation coil (FEC) which also known as hybrid excitation flux has additional advantage of high fixed flux compared to FEFSM which do not require PM but flux variable. Furthermore, the outer-rotor configuration of the machines can provides higher torque density and appropriate for in-wheel direct drive application. Based on 2-D finite element analysis (FEA), the design improvement has beenmade on the initial design machine shows that there is great enhancement on torque and power.**

I. INTRODUCTION

Electric motors with high torque density capability are essential for heavy applications such as in aerospace and automotive area[1]. Previously, permanent magnet (PM) brushless machines are widely used for these heavy applications due to their advantages of high torque capability. Nevertheless, due to the main flux source of PMs are located on the rotor, the machines are suffer from demagnetization effects which resulting in eddy current loss in the rotor. The main reason on this issue is difficulty to dissolve heat from the rotating part.

In recent years, flux-switching motors (FSMs) become an attractive research topic due to several advantages of higher torque density and efficiency. With all active components such as PM, DC field excitation coil (DC FEC), and armature coil are located on the stator, the machine is said very robust in which only consist single piece of rotor. Various applications of FSM have been reported, ranging from wind power generation, automotive, aerospace, power tools and etc [2-5]. Generally FSMs can be classified into three groups, namely permanent magnet (PM) FSMs, hybrid excitation (HE) FSMs, and field excitation (FE) FSMs as shown in Fig. 1. Both PMFSMs and FEFSMs have only single excitation flux source which come from PM and FE coil, respectively, while in HEFSM the magnetic flux source is generated from both the PM and FECs [6].

However, most of research have been reported are mainly focused on inner-rotor configuration [7-13]. It is quite difficult to find any report on outer-rotor FSM. Lately, a report on outer-rotor PMFSM has been published in 2010 and the target of the proposed machine is used for light traction EV applications [14-15]. Nonetheless, with single magnetic flux source of constant PM, it also may suffer from demagnetization effect and uncontrollable flux. Thus, this paper presents a design study on 12S-14P outer-rotor for hybrid excitation flux switching machine (HEFSM) and field-excitation flux switching machine (FEFSM) to meet the requirement of in-wheel drive electric vehicle (EV). Previously, the authors have proposed an outer-rotor HEFSM and FEFSM with 12Slot-10Pole configuration in which the initial design has been described in [16]-[17]. Based on 2-D analysis demonstrated, the proposed machine has good torque and power density capability to be applied on various speed condition of EV.

The rest of the paper is organized as follows; The FEA-based design investigation on the initial design machine of 12slot-14pole outer-rotor HEFSM and FEFSM is discussed in Section II. The improved design machine and the performance enhancement are explained in Section III. Finally, a short conclusion is explained in Section IV.

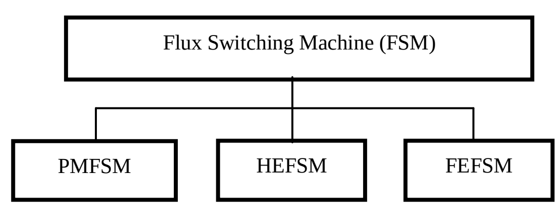

Fig. 1: Classification of flux switching machines

II. FEA-BASED PERFORMANCE ANALYSISON INITIAL DESIGNOF 12SLOT-14POLE HEFSM WITH OUTER-ROTOR CONFIGURATION

A. Finite Element Analysis (FEA) Design

Initially, the proposed 12slot-14pole HEFSM and FEFSM with outer-rotor configuration is designed using JMAG-Designer 13.0 software. This software is used as 2-D finite element solver along the design studies. The initial structure of the proposed machine is shown in Fig. 2 and the coil turns for armature coil and excitation coilare examined by equation (1).

$$N_a = \sqrt{\frac{\alpha_a R_a S_a}{4\rho L_{a-ave}}} \text{ and } N_e = \sqrt{\frac{\alpha_e R_e S_e}{4\rho L_{e-ave}}} \quad (1)$$

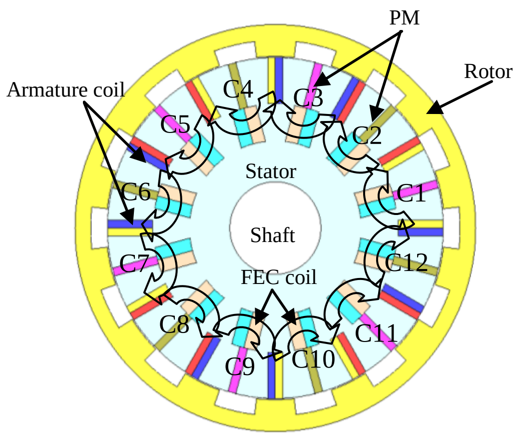

Fig. 2: Initial design 12slot-14pole outer-rotor HEFSM

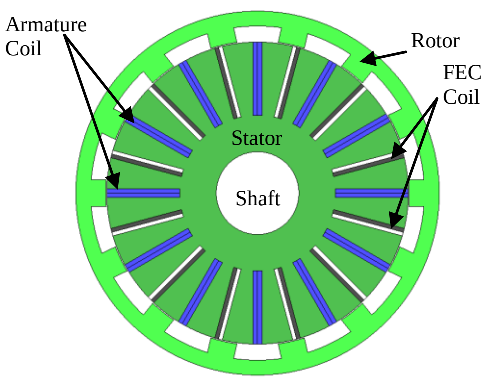

Fig. 3: Initial design 12slot-14pole outer-rotor FEFSM

Table I shows the proposed machine's specifications, conditions, and the calculated value of N_a, N_e, J_a and J_e.

TABLE I
THE INITIAL MACHINE'S SPECIFICATIONS

Armature		Excitation	
α_a	0.6/0.5	α_e	0.6/0.5
R_a	1 Ω	R_e	1 Ω
S_a	147.08 mm^2	S_e	197.51mm^2
ρ	1.673E-08 Ωm	ρ	1.673E-08 Ωm
N_a	7 turns	N_e	44 turns
J_a	30 A/mm^2	J_e	30 A/mm^2

From equation (1), subscript a and$e$ are representing armature coil and excitation coil components, respectively. N is the number of turns of coil winding, α is the filling factor, R is the coil resistance (Ω), S is the coil slot area (mm^2), and L is the average coil length (mm).

Furthermore, current density of armature coil (J_a) and current density of excitation coil (J_e) for the proposed machine can be determined by equation (2).

$$J_a = \frac{I_a N_a}{\alpha_a S_a} \text{ and } J_e = \frac{I_e N_e}{\alpha_e S_e} \quad (2)$$

B. Design Limitations and Conditions for outer-rotor 12S-14P HEFSM and FEFSM

The design limitations and conditions of the proposed outer-rotor HEFSM are set similar with the conventional interior permanent magnet synchronous motor (IPMSM) installed on Toyota Lexus RX400h as described in [17]. The torque and power of 333 Nm and 123 kW, respectively is set as the maximum target performances. On the other hand, the total PM volume is reduced to 1.0 kg in order to reduce the manufacturing cost. Furthermore, 30 A/mm^2 is set as the maximum current density of both armature coil and excitation coil, while the voltage and current limitation for the inverter is 650 V and 360 A_{rms}, respectively.

With all the active components are in rectangle shape make it easy for manufacture and all coils are non-overlap between armature coil and DC FEC that offer for shorter end winding. Consequently, the proposed machine is expected has low copper loss resulting for higher efficiency. Finally, the proposed machine is expected to have 11.1 Nm/kg and 4.1kW/kg of maximum torque and power density, respectively.In general, the variable parameters involve in this design are separated into stationary and rotating parts. On the stationary part, there are PM slot parameters, DC FEC slot parameters, and armature slot parameters, while on the rotating part only consist of rotor pole width, open rotor pole width and rotor pole depth.

In this study, the initial machine dimensions are depicted in Table 1.Furthermore, the material used in this study for PM is NEOMAX-35AH with the residual flux density and coercive force at 20ºc 1.2T and 932 kA/km, respectively, while the electromagnetic steel, 35H210 is used for the rotor and stator core

TABLE II
INITIAL MACHINE'S DIMENSION FOR HEFSM

Parameters	Initial Design
Inner radius of rotor (mm)	111.4
Depth of rotor pole (mm)	10.3
Width of rotor pole arc (º)	12.86
Depth of PM (mm)	30
Width of PM (mm)	2.63
Depth of FEC (mm)	23.88
Width of FEC (mm)	8.25
Depth of armature coil (mm)	28.35
Width of armature coil (mm)	4.95
Radius of shaft (mm)	30

TABLE III
INITIAL MACHINE'S DIMENSION FOR FEFSM

Parameters	Initial Design
Inner radius of rotor (mm)	110.36
Depth of rotor pole (mm)	10.82
Width of rotor pole arc (º)	11.35
Depth of FEC (mm)	53.04
Width of FEC (mm)	2.77
Depth of armature coil (mm)	53.04
Width of armature coil (mm)	3.17
Radius of shaft (mm)	30

C. Armature Coil Arrangement Test

Initially, it is essential to perform the operating principle of the proposed machine by conducting a coil arrangement test on each of the armature coil. The correct polarity and coil phase of armature coil must be examined and identified to confirm the proposed machine be able to operate properly. Firstly, the polarity of all the armature coils are set in counter clockwise direction, while the DC FEC and PM polarities are set in alternate direction in order to provide 12 north and 12 south poles, respectively. By injected zero current into DC FEC in which the FEC current density is 0 A/mm^2, the flux linkages on each armature coil are analyzed. Simultaneously, the generated magnetic fluxes on each armature coil are compared. Then, the fluxes profiles that have same pattern and phase angle are categorized into a same phase. The three-phase of 12 armature coils are examined based on normal balance three-phase 120º phase shifted.

From the coil arrangement test, it is found that the armature coils labeled as C1, C4, C7 and C10 represent the V-flux, while the armature coils labeled as C2, C5, C8, and C11 represent the U-flux, and armature coils labeled as C3, C6, C9, and C12 represent for W-flux of the machine as shown in Fig. 2. The fluxes linkage with the same phase are then combined into one phase making a three phase flux as illustrated in Fig. 3. All the generated flux are considered sinusoidal and has a maximum amplitude of 0.011 Wb. Thus, the three phase system and principle operation of the proposed machine has been performed through coil arrangement test.

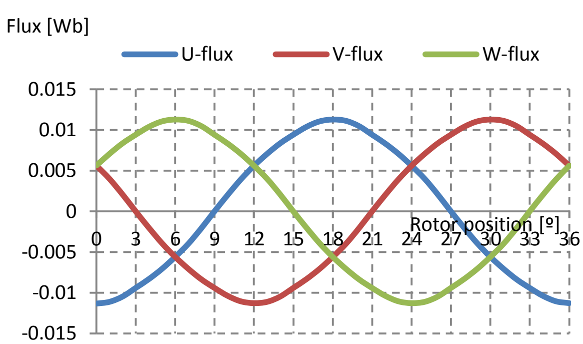

Fig. 4: Three-phase flux linkage generated by PM

D. Flux Path at 9°, 18º, 27º and 0/36º.

The flux path due to PM source for HEFSM is also investigated at different rotor position. Fig. 4 shows the flux path of PM at 0º and 9º rotor position. It is obvious that, 50% of the PM flux flows from stator to rotor while the remaining flux flows around the DC FEC slot to form a complete 12 cycles of flux. However, very high flux density occurs between the adjacent of FEC slot and between the lower edge of armature coil and upper edge of DC FEC slots which results in flux saturation. Therefore, the appropriate distance between them needs to be examined to minimize the flux saturation effect.

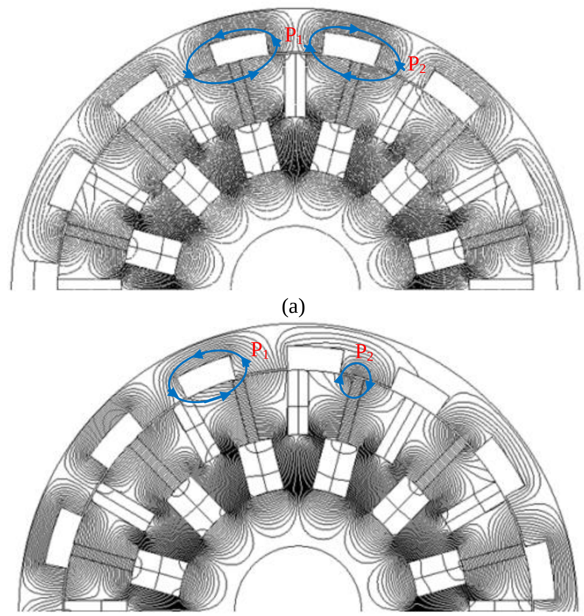

(b)

Fig. 5: Open circuit field distribution of the proposed motor (a) 0º rotor position (b) 9º rotor position

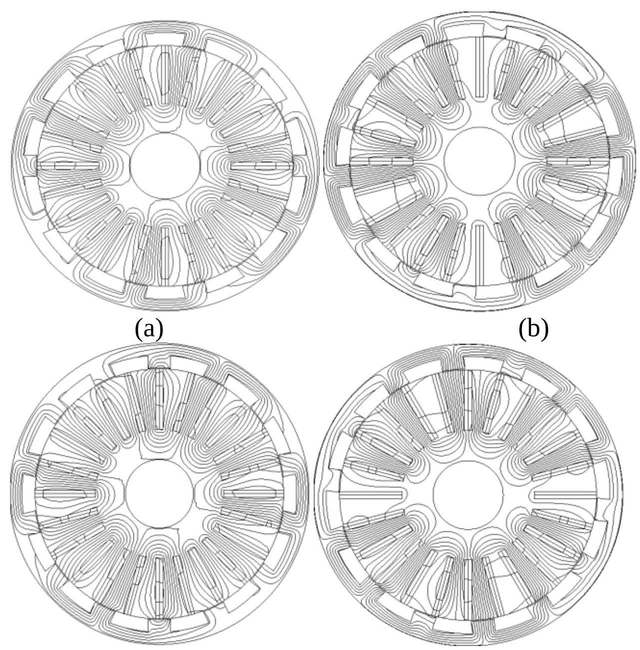

(a) (b)

(c) (d)

Fig. 6: Flux path for 12S-14P outer-rotor FEFSM motor (a) 0º/36º rotor position (b) 9º rotor position (c) 18° rotor position (d) 27º rotor position

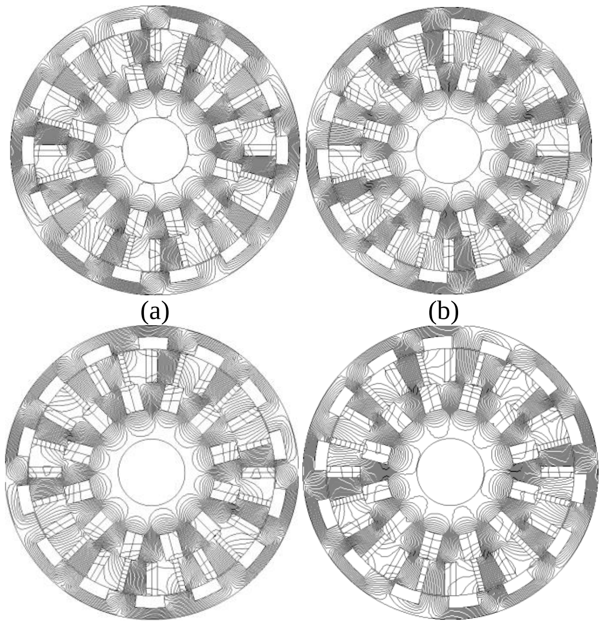

Fig. 7: Flux path for 12S-14P outer-rotor HEFSM motor (a) 0º/36º rotor position (b) 9º rotor position (c) 18° rotor position (d) 27º rotor position

E. Flux Distribution

This test shows about the flux distribution around the motor. It is classified into many types of color in determining its density. The highest value of the parameter is the one that being set during the plot. From the Figure 8, the highest set value is 2.4T while the maximum value during the operation of the motor is 2.3199T. The condition for this flux distribution is when current density, Je=30A/mm^2 and Ja=30A$_{rms}$/mm^2 . As for 12S-14P of outer-rotor HEFSM highest is set to 2.3T and with maximum value get is 2.88T.

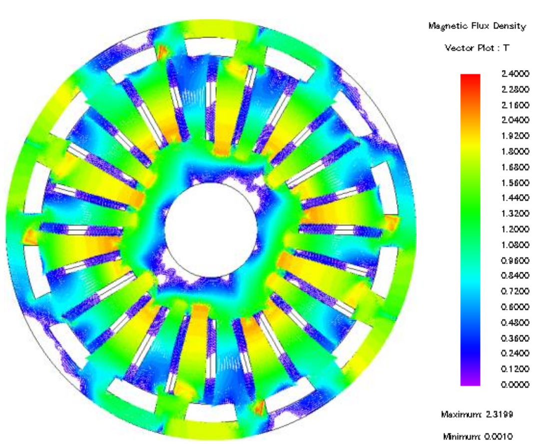

Fig. 8.Illustration of flux distribution of the outer-rotor 12S-14P FEFSM

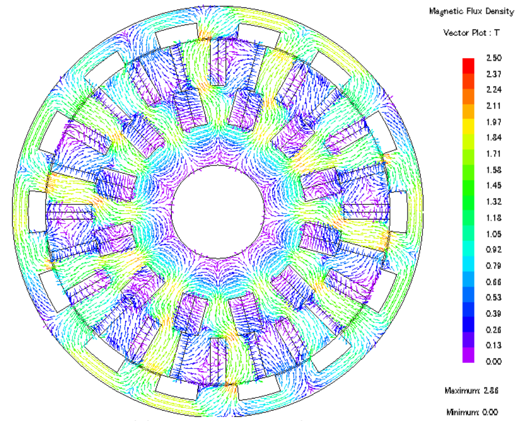

Fig. 9.Illustration of flux distribution of the outer-rotor 12S-14P HEFSM

F. Cogging Torque

The cogging torque of the proposed machine in open circuit condition is illustrated in Fig. 9. It is observed in 36º of rotor position which is one electric cycle; there is six cycles of peak-to-peak cogging torque. From the figure, it is clearly shown that the cogging torque is considered low because the cogging is less than 10 percent of the maximum torque get with the maximum peak-to-peak is approximately 7.99 Nm for HEFSM while 4.11Nm for FEFSM . Thus, the cogging torque has ability to be reduced by conducting design optimization and improvement of the motor especially on the distance of armature coil and DC FEC slot.

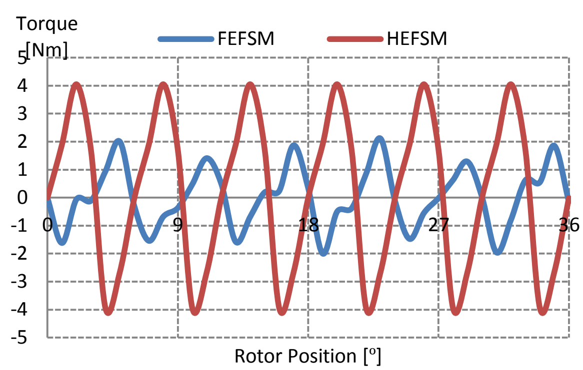

Fig. 9.Illustration of flux distribution of the outer-rotor 12S-14P FEFSM

G. Flux Characteristics at Various Current Densities

The flux linkage of PM and various DC FEC current densities are demonstrated in Fig. 10. It is obvious that when DC FEC current density, J_e start increased, the flux linkage also increasing and reach to maximum when Je set to 10 A/mm^2. The maximum flux linkage at this condition is approximately 0.051 Wb which is increased more than three times when compared with flux linkage come from PM only. When further increased of J_e, the flux linkage starts to reduce and finally when J_e is set to maximum of 30 A/mm2, the magnitude of flux linkage is approximately 0.028 Wb. This phenomenon is expected due to flux saturation when higher J_e is injected to the system beyond 10 A/mm^2. However, this analysis has proved that the additional DC FEC can improve the generated flux from PM and offers variable flux control capability.

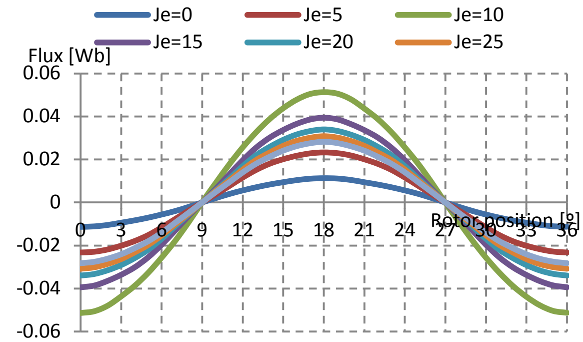

(a)

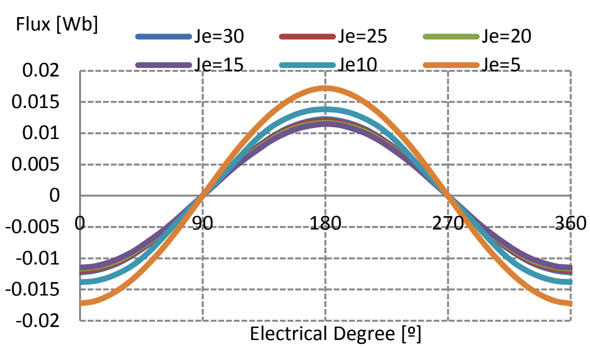

(b)

Fig. 10: Flux linkage at various DC FEC current densities

H. *Torque Characteristic at Various Current Densities*

The torque characteristics at various armature current density and DC FEC current density are also investigated. The results obtained is plotted in Fig. 11 and Fig. 12, in which the armature coil and DC FEC current densities are varied from 0 to 30 A/mm^2.

The graph show that the maximum average torque of 243.52 Nm of initial design machine for HEFSM is obtained when armature and FEC current densities are set to 30 Arms/mm^2 and 25 A/mm^2 while the average torque at the same condition for FEFSM is 112.95 Nm, respectively, whereas the maximum power obtained for the initial design machine HEFSM is 83.03 kW and 72.10kW for FEFSM. These results indicate that the torque and power of the machine can be controlled by varying the current densities of DC FEC and armature coil.

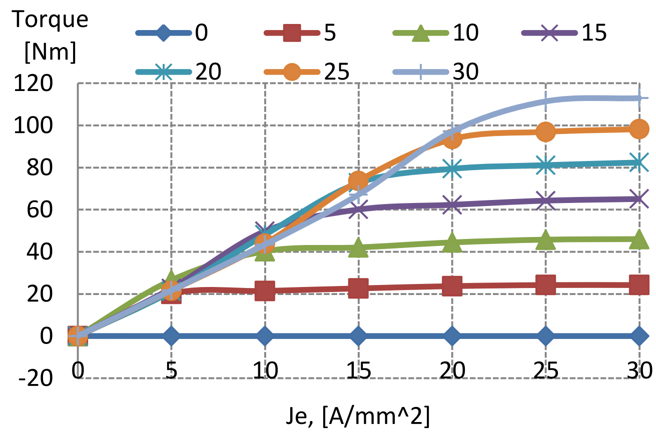

Fig. 11: Torque versus FEC current dentisy at various armature current density for FEFSM

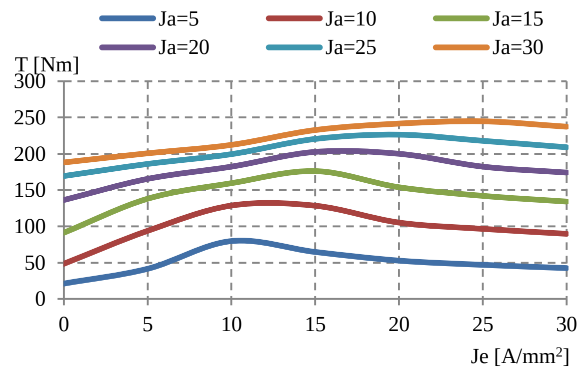

Fig. 12: Torque versus FEC current dentisy at various armature current density for HEFSM

IV. Conclusion

This paper has discussed and demonstrated the initial design of 12slot-14pole outer-rotor HEFSM and 12Slot-14pole outer-rotor FEFSM. The research goal is to determine the initial result such as flux linkage, cogging torque, average and maximum torque, flux line and power has been achieved. It can be concluded that a HEFSM initial result have a higher average torque and power, hence suitable for a high torque application such as HEV. As for the flux distribution, HEFSM is higher and smoothly distributed compared to FEFSM. The main factor of a motor such as HEFSM is the permanent magnet contained at the stator because it produce its on magnetic flux and increase the average torque respectively. For the cogging torque, average torque and power, it can be improve in future through optimization process although it still in initial value. Therefore, further design investigation and improvement will be conducted in order to achieve a better performance of torque and power.

V. ACKNOWLEDGMENT

The authors would like to acknowledge The Ministry of Higher Education Malaysia (MOHE) and Universiti Tun Hussein Onn Malaysia (UTHM) for the financial support of this research study.

VI. REFERENCES

[1] Z. Q. Zhu and D. Howe, 2007. Electrical machines and drives for electric, hybrid, and fuel cell vehicles, Proc. IEEE, vol.95, no. 4, pp. 746-765, 2007.

[2] Y. Amara, E. Hoang, M. Gabsi, and M. Lecrivain, 2005. Design and comparison of different flux-switching synchronous machines for an aircraft oil breather application, Euro. Trans Electr. Power, no. 15, pp. 497-511.

[3] C. Pollock, H. Pollock, R. Borron, J. R. Coles, D. Moule, A. Court, and R. Sutton, 2006. "Flux-switching motors for automotive applications, IEEE Trans. Ind. Appl., vol. 42, no. 5, pp. 1177-1184.

[4] M. J. Jin et al, 2010. Cogging torque suppression in a permanent magnet flux-switching integrated starter generator, IET Electric Power Appl., vol 4, no. 8, pp. 647-656, Aug 2010.

[5] H. Pollock, C. Pollock, R.T. Walter, and B.V. Gorti, 2003. Low cost high power density, flux switching machines and drives for power tools, in Proc. IEEE Industry Applications Soc. Annu. Meeting, pp. 1451-1457.

[6] E. Sulaiman, T. Kosaka, and N Matsui, 2011. High power density design of 6slot-8pole hybrid excitation flux switching machine for hybris electric vehicles, IEEE Trans. on Magn. vol.47, no. 10, pp.4453-4456, Oct 2011.

[7] C. Pollock and M. Brackley, 2003 Comparison of the acoustic noise of flux-switching and switched reluctance drive, IEEE Trans. Ind. Appl., vol.39, no. 3, pp. 826-834.

[8] W. Xu, J. Zhu, Y. Zhang, Y. Wang, Y. Li, and J. Hu, 2010. Flux-switching permanent magnet machine drive system for plug-in hybrid electrical vehicle, Proc. of IEEE Conf. on Australian Universities Power Engineering (AUPEC), pp. 1-6.

[9] J.T. Chen and Z.Q. Zhu, 2010. Winding configuration and optimal stator rotor pole combination of flux-switching PM brushless machines, IEEE Trans. on Energy Conversion, vol. 25, pp. 293-302.

[10] Y. Wang and Z. Deng, 2012. Comparison of hybrid excitation topologies for flux-switching machines, IEEE Trans. on Magn., vol. 48, no. 9.

[11] Y. Tang, J.J.H. Paulides, T.E. Motoasca, and E.A. Lomonova, 2012. Flux-switching machine with DC excitation, IEEE Trans. on Magn., vol. 48, no. 11.

[12] E. Sulaiman, T. Kosaka, and N. Matsui, 2011. Design Optimization of 12Slot-10Pole hybrid excitation flux switching synchronous machine with 0.4 kg permanent magnet for hybrid electric vehicles, Proc. of International IEEE Conference on Power Electronics and ECCE Asia (ICPE & ECCE), pp. 1913-1920.

[13] W.Fei, P.C.K. Luk, J. Shen, and Y. Wang, 2009. A Novel Outer-Rotor Permanent-Magnet Flux-Switching Machine for Urban Electric Vehicle Propulsion, in 3rd International Conference on Power Electronics Systems and Applications (PESA), pp. 1–6.

[14] Y. Wang, M.J. Jin, J. Shen, W.Z. Fei, and P.C.K. Luk, 2010. An outer-rotor permanent magnet flux-switching machine for traction application, Energy Conversion Congress and Expo-sition (ECCE), pp. 1723-1730.

[15] W. Fei, P. Chi, K. Luk, S. Member, J. X. Shen, Y. Wang, and M. Jin, 2012. A Novel Permanent-Magnet Flux Switching Machine With an Outer-Rotor Configuration for In-Wheel Light Traction Applications, IEEE Transactions on Industry Applications, vol. 48, no. 5, pp. 1496–1506.

[16] M.Z. Ahmad, E. Sulaiman, Z.A. Haron, and T. Kosaka, 2012. Preliminary Studies on a New Outer-Rotor Permanent Magnet Flux Switching Machine with Hybrid Excitation Flux for Direct Drive EV Applications, IEEE Int. Power and Energy Conference (PECON2012), pp. 928-933.

[17] S.M.N.S. Othman, E. Sulaiman 2014. Design study of 3-phase field-excitation flux switching motor with outer-rotor configuration, IEEE Power Engineering and Optimization Conference (PEOCO 2014).

[18] E. Sulaiman, T. Kosaka, N. Matsui, and M. Z. Ahmad, 2012. Design Studies on High Torque and High Power Density Hybrid Excitation Flux Switching Synchronous Motor for HEV Applications, in IEEE International Power Engineering and Optimization Conference (PEOCO), pp. 333–338